Dispersive shock waves propagating in the cubic-quintic derivative nonlinear Schrödinger equation

E. Kengne, A. Lakhssassi, T. Nguyen-Ba, and R. Vaillancourt

Abstract: The propagation of a dispersive shock wave is studied in a quintic-derivative nonlinear Schrödinger (Q-DNLS) equation, which may describe, for example, the wave propagation on a discrete electrical transmission line. It is shown that a physical system described by a Q-DNLS equation without a dissipative term may support the propagation of shock waves. The influence of the derivative nonlinearity terms on the shock is analyzed. Using the found exact shock solutions of the Q-DNLS equation as the initial input signal, we investigate numerically the spatiotemporal stability of the shock signal in the network.

PACS Nos: 42.65.Tg, 42.25.Bs, 84.40.Az, 02.60.Cb

Résumé : Nous étudions la propagation d'une onde de choc dispersive à l'aide d'une équation différentielle quintique non linéaire de Schrödinger (équation Q-DNLS), qui peut décrire, par exemple, la propagation d'onde sur une ligne de transmission électrique discrète. Nous montrons qu'un système physique décrit par une équation Q-DNLS sans terme dissipatif peut permettre la propagation d'onde de choc. Nous étudions l'influence des termes non linéaires en dérivée sur l'onde de choc. Utilisant comme signal de départ, la solution exacte pour l'onde de choc obtenue de l'équation Q-DNLS, nous étudions la stabilité spatiotemporelle du signal de choc dans la ligne.

[Traduit par la Rédaction]

1. Introduction

Since the pioneering works by Hirota and Suzuky [1] on electrical transmission lines simulating the Toda lattice, a growing interest has been devoted to the use of the nonlinear transmission lines (NLTLs), in particular, for studying nonlinear wave propagation. In fact, NLTLs are convenient tools for studying wave propagation in nonlinear dispersive media. In particular, they provide a useful way to check how the nonlinear excitations behave inside a nonlinear medium and to model the exotic properties of new systems [1–17]. Theoretical studies on the NLTLs show that the system of equations governing the physics of the network can be reduced to a complex cubic/cubic-quintic Ginzburg–Landau equation (with or without a derivative in the cubic term) or a pair of coupled Ginzburg–Landau equations (see for example refs. 15, 18, 19).

Most recently, Kengne and Liu [20] presented a model for wave propagation on a discrete electrical transmission line based on the modified complex Ginzburg–Landau (MCGL) equation, derived in the small-amplitude and long-wavelength limit using the standard reductive perturbation technique and complex expansion [21] on the governing nonlinear equations. This MCGL equation is also referred to as the "derivative-nonlinear Schrödinger (Q-DNLS) equation" or the "real cubic-quintic Ginzburg–Landau equation" and can take the form

$$i\frac{\partial u}{\partial t} - P\frac{\partial^2 u}{\partial x^2} - \gamma u - Q_1|u|^4 u - i\left[(Q_2 + 2Q_3)|u|^2\frac{\partial u}{\partial x} + Q_3 u^2\frac{\partial u^*}{\partial x}\right] = 0 \quad (1)$$

where P, γ, and q_j (j = 1, 2, 3) are real transmission line parameters, and u^* stands for the complex conjugate of u. The two terms $|u|^2(\partial/\partial)u$ and $u^2(\partial/\partial)u^*$ in (1) are called derivative nonlinear terms, and appear in the asymptotic derivation. Their coefficients $Q_2 + 2Q_3$ and Q_3 represent the relative magnitudes of the nonlinear dispersion. Because all parameters of (1) are real, we henceforth call it the "quintic-derivative nonlinear Schrödinger equation". Deissler and Brand [22] showed numerically that these two terms can significantly slow down the propagating speed of the pulses and also cause the nonsymmetry of pulses. Because γ is a real number, the term γu can be removed from (1) using the substitution $u(x, t) = w(x, t)\exp(-i\gamma t)$. Thus, without loss of generality, we henceforth suppose that $\gamma = 0$ Modulational instability of partially coherent signals in electrical transmission lines that are governed by the Q-DNLS equation (1) is investigated in ref. 23, and the following condition on the modulational instability has been found:

$$PQ_1 > 0 \quad (2)$$

It has been shown that the derivative nonlinearity Q_3 decreases the instability region, while the higher order nonlinearity coefficient Q_1 tends to increase the instability region.

Received 15 October 2009. Accepted 21 December 2009. Published on the NRC Research Press Web site at cjp.nrc.ca on 12 February 2010.

E. Kengne[1] **and A. Lakhssassi.** Département d'informatique et d'ingénierie, Université du Québec en Outaouais, 101 St-Jean-Bosco, Succursale Hull, Gatineau, QC J8Y 3G5, Canada.
T. Nguyen-Ba and R. Vaillancourt. Department of Mathematics and Statistics, Faculty of Science, University of Ottawa, 585 King Edward Ave., Ottawa, ON K1N 6N5, Canada.

[1]Corresponding author (e-mail: ekengne6@gmail.com).

Fig. 1. Velocity η of the shock wave (1) and group velocity Ω_K (2) versus (*a*) the derivative nonlinearity Q_3 for $P = 0.4$, $Q_1 = 0.2$, $Q_2 = 1.3$ and (*b*) versus the derivative nonlinearity Q_2 for $P = 0.4$, $Q_1 = 0.2$, $Q_3 = 0.7$.

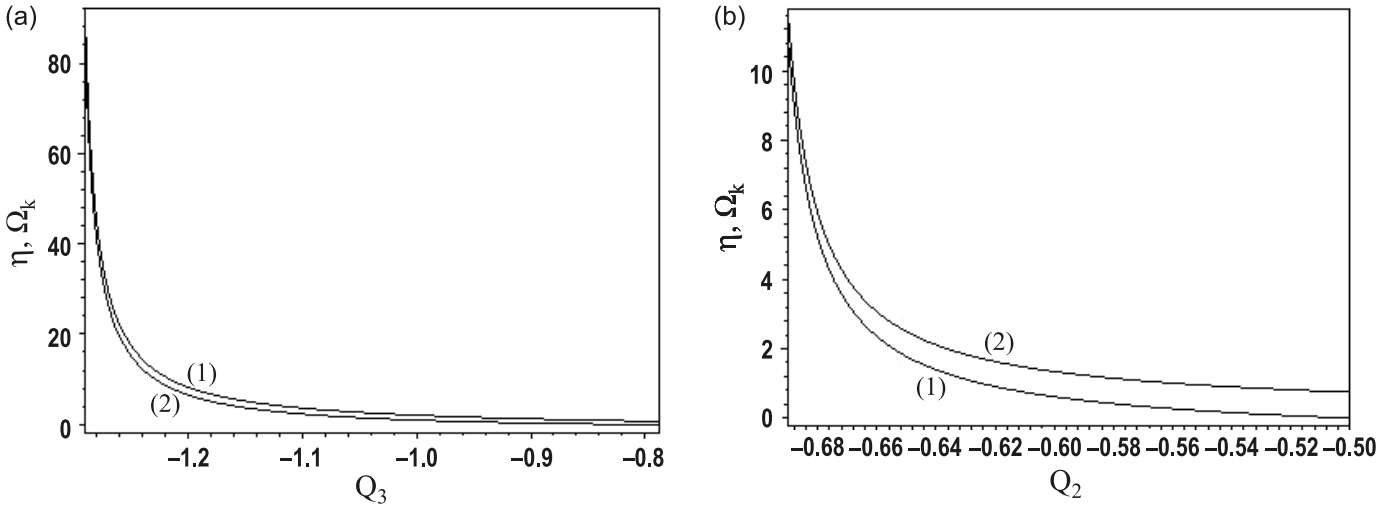

Fig. 2. Plots (1) of V and (2) ρ versus the derivative nonlinearity Q_3 (*a*), and dependence of V on ρ (*b*) for $P = 1$ and $Q_1 = –0.5$. (plotted quantities are dimensionless).

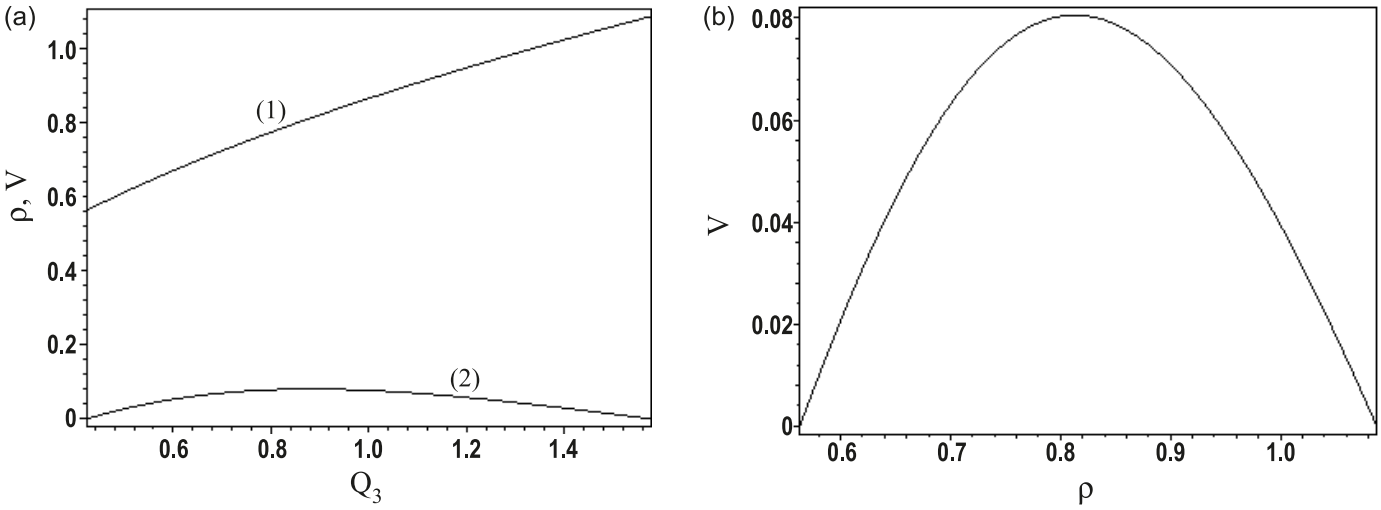

The Q-DNLS equation (1) is a well-known dynamical model with numerous physical applications ranging from nonlinear optics to the theory of molecular vibrations. The Q-DNLS equation demonstrates a rich variety of dynamical behaviors, including bright and dark solitary waves and shock waves (SWs), that is, sharp expanding fronts followed by localized excitations and background oscillations.

Dispersive shock waves (DSWs), also called unsteady undular bores [24, 25], are nonlinear wave-like structures, which are generated in the breaking profiles of large-scale nonlinear waves propagating in dispersive media. The DSWs have been observed experimentally or their existence has been theoretically predicted in various nonlinear media — water [26], plasma [27], optical fibers [28], lattices [29], and more recently in Bose–Einstein condensates [30, 31]. In contrast to the usual dissipative shocks where the combined action of nonlinear and dissipation effects leads to sharp jumps of the wave intensity, accompanied by abrupt changes in other wave characteristics, in dispersive shocks the viscosity effect is either absent or negligibly small compared with the dissipative one, and, instead of intensity jumps, the combined action of nonlinear and dispersion effects leads to the formation of an oscillatory wave region (for a review, see, for example, ref. 32). Dispersive shock waves (DSWs) have yielded novel dynamics and interesting interaction behavior that has only recently begun to be studied theoretically (see, for example, ref. 33). It is well known (see, for example, ref. 26) that if the initial pulse is strong enough, so that the nonlinear term dominates over the dispersive one in the initial stage of the pulse evolution, then the dispersive shock wave develops after the wave breaking point.

The aim of this paper is to show the possibility for a shock wave to propagate in a system described by a Q-DNLS equation without a dissipative term. If Deissler and Brand [22] have shown that the derivative nonlinear terms of a complex Ginzburg–Landau equation can significantly slow down the propagating speed of the pulses and also cause the nonsymmetry of pulses, we show in this work that these two terms for a Q-DNLS equation also cause the propagation of a dispersive shock wave.

The paper is organized as follows. In Sect. 2, we find two

Fig. 3. Velocity V of the shock (1) and asymptotic continuous wave amplitude ρ (2) versus the parameter Q_3 (*a*) and dependence of V on ρ (*b*). The equation parameters are taken to be $P = 1$ and $Q_1 = -0.5$, while the derivative nonlinearities are related by $Q_2 + 3Q_3 = 0$ (plotted quantities are dimensionless).

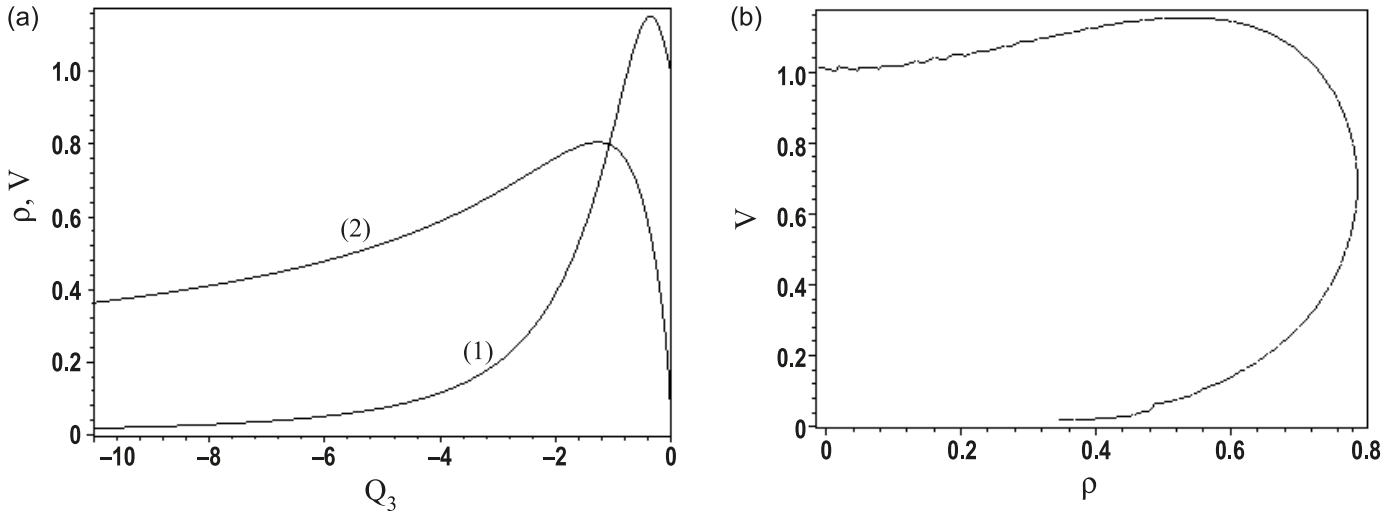

classes of exact stationary-phase modulated-shock-wave solutions of (1); the first class contains the solutions with one free parameter, while the second class consists of either two-parameter solutions or zero-parameter solutions. In Sect. 3, we investigate numerically the stability of the shock. Section 4 concludes the paper.

2. Dispersive-shock-wave solutions of the Q-DNLS equation (1)

The shock-wave type solutions of the Q-DNLS equation (1) can be sought in the generic form

$$u(x,t) = a(\xi)\exp\left[i\left(\psi(\xi) - \omega t\right)\right] \tag{3}$$

where $\xi = x - vt$ and the phase function $\psi(\xi)$ is in general a function of amplitude $a(\xi)$.

2.1. Class of one-parameter solutions

Following Nozaki and Bekki [34], we seek the first class of the shocklike solution of (1) in the form

$$u(x,t) = \frac{a\exp\left[i(Kx - \Omega t)\right]}{\{1 + \exp\left[-2\mu(x - \eta t)\right]\}^{(1/2)+i\alpha}}, \qquad \mu a \neq 0 \tag{4}$$

where a, K, Ω, μ, η, and α are real parameters. Inserting relation (4) into (1) results in the following set of equations.

$$\begin{aligned}
&Q_1 a^4 - K(Q_2 + Q_3)a^2 - (\Omega + K^2 P) = 0\\
&\eta + 2P(K + 2\alpha\mu) = 0\\
&\eta + (Q_2 + 3Q_3)a^2 + 2P(K - 2\alpha\mu) = 0\\
&P(\mu^2 - K^2) - \Omega - 2\eta\alpha\mu - 4P\mu\alpha(K + \alpha\mu) = 0\\
&2\Omega + 2P(K^2 + \mu^2) + 2\eta\alpha\mu + 4KP\alpha\mu\\
&\quad - a^2 Q_3(K + 2\alpha\mu) + a^2(K + 2\alpha\mu)(Q_2 + 2Q_3) = 0
\end{aligned} \tag{5}$$

It is important to notice that a necessary condition for system (5) under condition $\mu a \neq 0$ to admit a nontrivial solution is that $|Q_3| + |Q_2 + 2Q_3| > 0$. This means that the derivative nonlinear terms in (1) are responsible for the dispersive shock-wave propagation in the network.

Solving system (5), we obtain

$$\begin{aligned}
K &= \frac{8PQ_1 - Q_3(Q_2 + 3Q_3)}{6P(Q_2 + Q_3)}a^2\\
\eta &= -\frac{16PQ_1 + (Q_2 + 3Q_3)(Q_3 + 3Q_2)}{6(Q_2 + Q_3)}a^2\\
\mu^2 &= -\frac{16PQ_1 + (Q_2 + 3Q_3)(Q_3 + 3Q_2)}{48P^2}a^4\\
\alpha &= \frac{(Q_2 + 3Q_3)}{8P\mu}a^2\\
\Omega &= \left[\left(6[Q_3(Q_2 + 3Q_3) - 2PQ_1](Q_2 + Q_3)^2\right.\right.\\
&\quad \left.\left. - [8PQ_1 - Q_3(Q_2 + 3Q_3)]^2\right)/\left(36P(Q_2 + Q_3)^2\right)\right]a^4
\end{aligned} \tag{6}$$

a being a free real parameter. Since $\mu^2 > 0$, the transmission line parameters P and Q_j ($j = 1, 2, 3$) must satisfy the relationship

$$16PQ_1 + (Q_2 + 3Q_3)(Q_3 + 3Q_2) < 0 \tag{7}$$

Inequality (7) is then the condition under which the propagation of shock waves is possible on the NLTLs. Hence, the SW exists only with both positive and negative velocity η, depending on the sign of $Q_2 + Q_3$ (see the second equation in (6)). It should be noted that condition $Q_2 + Q_3 \neq 0$ follows from our assumption $\mu \neq 0$ (see (5)). It follows from (2) and inequality (7) that the motion of shock waves is possible in the modulational instability domain only when the derivative nonlinearity coefficients $Q_2 + 2Q_3$ and Q_3 satisfy the relationship

$$\frac{Q_2 + 2Q_3}{Q_3} - 2 < 0 \tag{8}$$

As we can see from (6), SWs in the Q-DNLS equation move at a constant velocity that explicitly depends on the dispersive coefficient P, on the higher order nonlinearity coefficient Q_1, and on the two derivative nonlinearity coeffi-

Fig. 4. Wave evolutions in the modulational instability region. The initial condition is taken from the first class of shock-wave solutions with $P = 0.4$, $Q_1 = 0.2$, $Q_2 = 1.3$, and $Q_3 = -1$. Plots of rows (*a*) and (*b*) show the wave evolutions at given times along the *x*-direction and at given point along the *t*-direction, respectively. Here, we used $a = 1$.

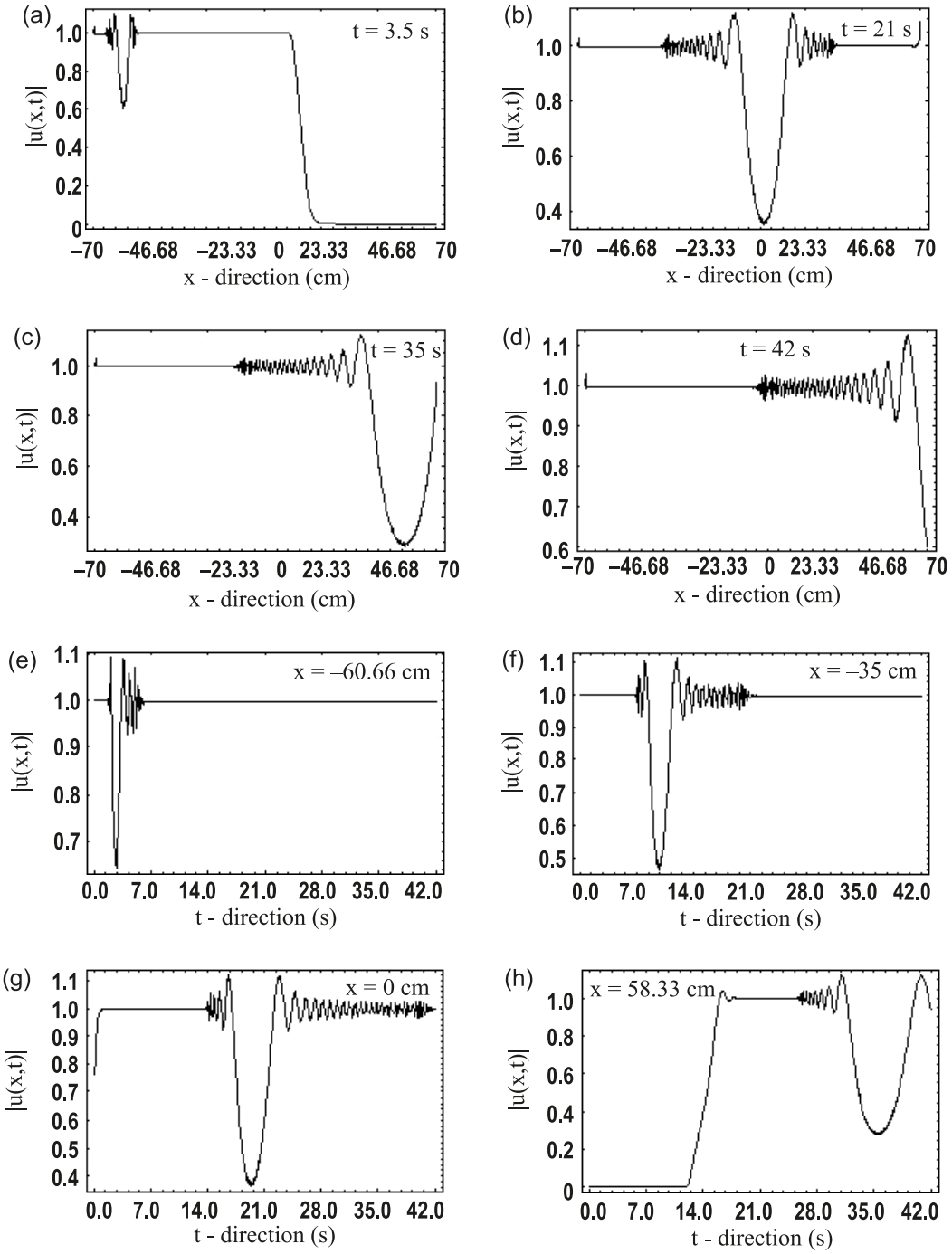

cients Q_2 and Q_3. Using (6), one obtains the following group velocity:

$$\frac{\partial \Omega}{\partial K} = -2KP - \frac{(Q_2 + Q_3)a^2}{4} = -\frac{32PQ_1 + 3Q_2^2 + 2Q_2Q_3 - 9Q_3^2}{12(Q_2 + Q_3)}a^2 \quad (9)$$

In Fig. 1, we plot the shock-wave velocity (1) and the group velocity (2) as functions of derivative nonlinearity. Figure 1*a* shows the plot versus Q_3 for the equation parameters $P = 0.4$, $Q_1 = 0.2$, $Q_2 = 1.3$, while Fig. 1*b* corresponds to the plot versus Q_2 for the parameters $P = 0.4$, $Q_1 = 0.2$, $Q_3 = 0.7$. The plots in Fig. 1 show that the shock-wave velocity as the group velocity decreases as the derivative nonlinearities increase. We can then conclude that the two derivative nonlinearity terms can significantly slow down the propagating speed of the shock wave. Figure 1*a* shows that the shock-wave velocity is always greater than the group velocity and this suggests that there may exist many

Fig. 5. Wave propagation in the modulational stability region with equation parameters $P = 0.4$, $Q_1 = -0.2$, $Q_2 = 1.3$, and $Q_3 = -1$ The initial condition has been taken from the first class of shock-wave solutions with $a = 1$. Plots of rows (*a*) and (*b*) show the wave evolutions at given times along the *x*-direction and at given point along the *t*-direction, respectively.

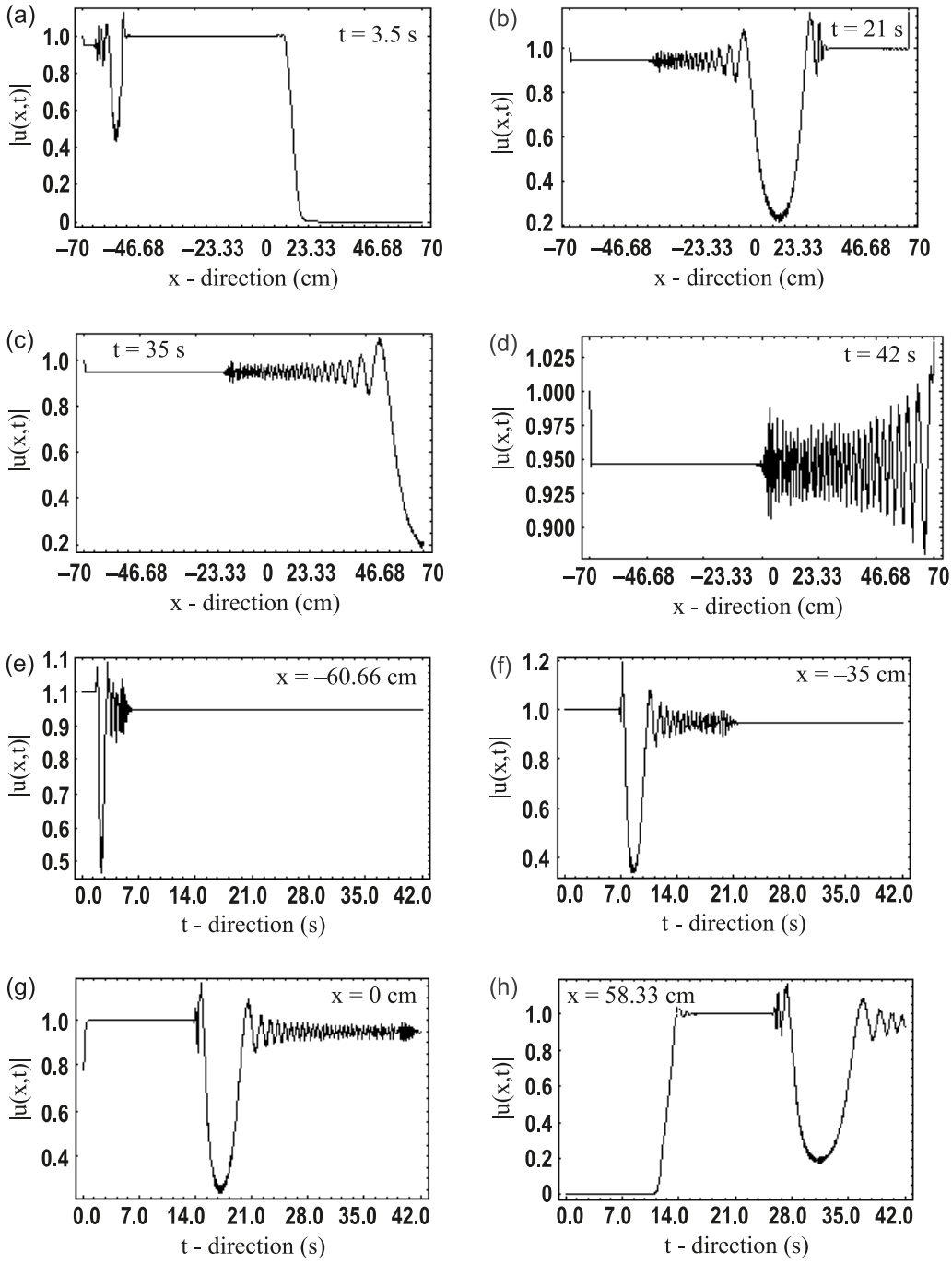

types of structures evolving behind the shock wave for the given equation parameters for $-1.29 \leq Q_3 \leq -0.78757$. As can be seen from Fig. 1*b*, the group velocity is always greater that the front's speed, meaning that for the given set of equation parameters and for $-0.69 \leq Q_2 \leq -0.5$, there may exist many types of structures evolving in front the shock wave.

2.2 Class of zero-parameter and two-parameters solutions

For both zero-parameter and two-parameters solutions, it is preferable to write solution (3) in the following generic form:

$$u(x,t) = R(x - Vt = z)\exp\left(i\int_0^z \Phi(z)\mathrm{d}z - i\rho^2 t\right) \qquad (10)$$

Fig. 6. Wave evolution in the modulational stability region with equation parameters $P = 0.4$, $Q_1 = -0.2$, $Q_2 = 1.3$, and $Q_3 = -3$. Plots of rows (*a*) and (*b*) show the wave evolutions at given times along the *x*-direction and at given point along the *t*-direction, respectively.

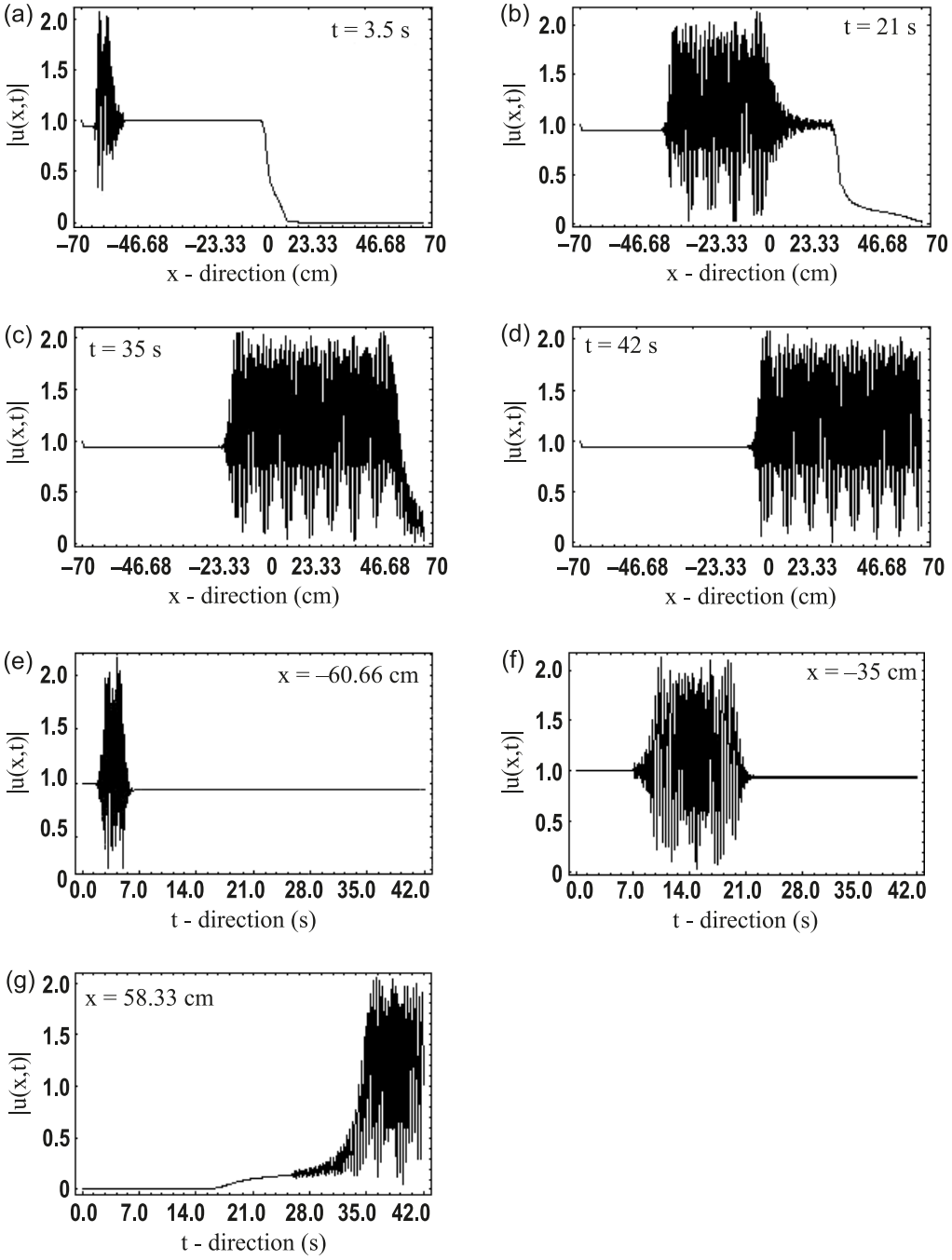

where V is the SWs velocity, $R(z)$ is the real amplitude with boundary values $R(-\infty) = 0$, $R(+\infty) = \sqrt{2\rho}$, ρ being the asymptotic continuous wave amplitude, and $\Phi(z)$ takes the boundary values $\Phi(\pm\infty) = -[(Q_2 + 3Q_3)\rho^2 + V](2P)^{-1}$. We limit ourselves to the shock waves with positive velocity ($V > 0$) corresponding to a situation where the zero-state domain expands into the energy-carrying one. As in Sect. 1, we will see below that dispersive shock-wave propagation in the network is possible only if $|Q_3| + |Q_2 + 2Q_3| > 0$ that is, in the presence of at least one derivative nonlinear term in (1).

Inserting (10) into (1) and taking the boundary conditions into account, we obtain

$$R'' + \frac{(P+1)V - 2\rho^2 P}{2P^2}R + \frac{(P+2V+1)Q_2 + (3P+2V+3)Q_3}{4P^2}R^3 + \frac{4PQ_1 + 4Q_2Q_3 + Q_2^2 + 3Q_3^2}{4P^2}R^5 = 0 \quad (11)$$

Fig. 7. Wave profile in the modulational instability region. The initial condition is taken from the first class of shock-wave solutions with $P = 0.4$, $Q_1 = 0.2$, $Q_2 = 1.3$, and $Q_3 = -3$. Plots of rows (*a*) and (*b*) show the wave evolutions at given times along the *x*-direction and at given point along the *t*-direction, respectively.

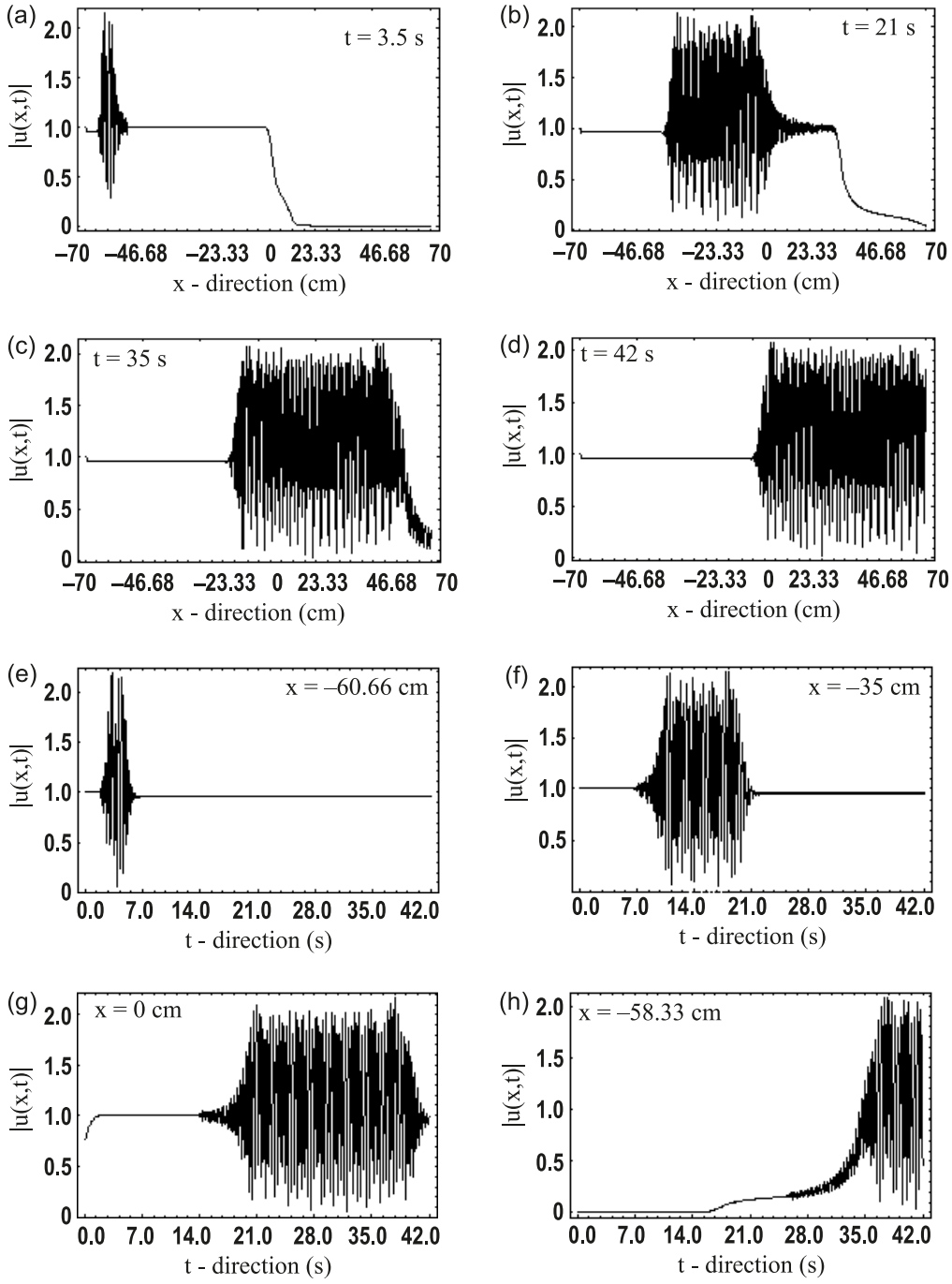

$$\Phi(z) = -\frac{V}{2P} - \frac{Q_2 + 3Q_3}{4P} R^2(z) \tag{12}$$

Equation (11) makes its presence felt in many contexts: it appears as a reduction equation of various nonlinear equations such as the Rangawala–Rao equation, the Ablowitz equation, and the Gerdjikov and Ivanov equation (see Kong [35] and Dey et al. [36] for references). Many new solitary wave solutions are obtained by mapping this equation into the field equation of ϕ^6 as in field theory (see Behera and Khare [37]).

The shock-wave solution of (11) is sought in the form

$$R(z) = \rho\sqrt{1 + \tanh mz} \tag{13}$$

where m is a real parameter. If we substitute (13) into (11),

Fig. 8. Wave evolution in modulational stability region for equation parameters $P = 2$, $Q_1 = -27$, $Q_2 = -2$, and $Q_3 = 2$. Plots of rows (*a*) and (*b*) show the wave evolutions at given times along the *x*-direction and at given point along the *t*-direction, respectively.

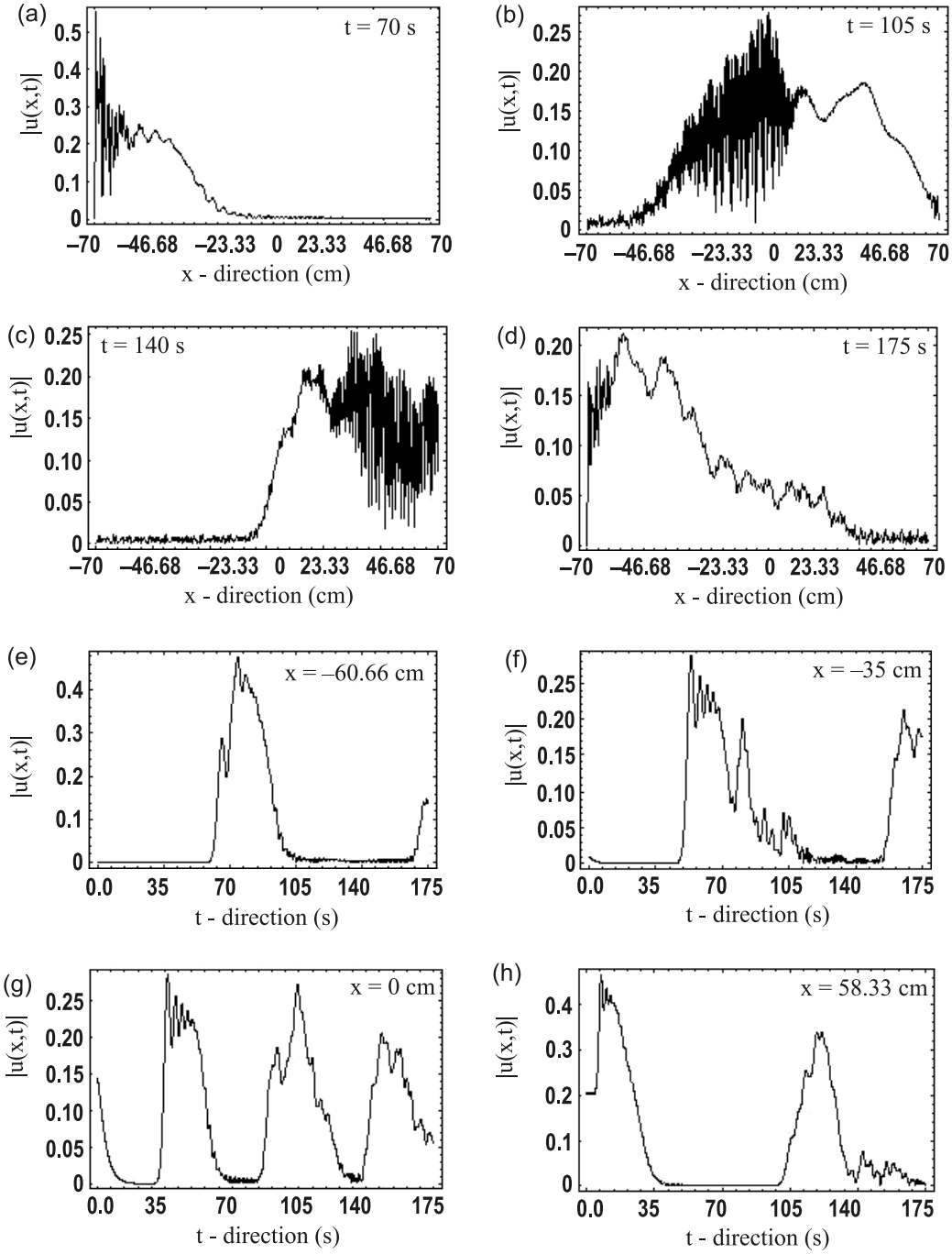

we can obtain, after long calculations a system of equations in V, m, and ρ. The different cases when the equation is solvable are analyzed below.

1. Case $Q_2 + Q_3 = 0$

When

$$Q_2 + Q_3 = 0, \qquad PQ_1 < 0, \qquad (P+1)Q_3 > 0 \tag{14}$$

one obtains

$$m^2 = -\frac{3[Q_3(P+1)]^2}{64P^3Q_1}, \qquad \rho^2 = -\frac{3(P+1)Q_3}{16PQ_1},$$
$$V = \frac{3Q_3[4P-(P+1)Q_3]}{2(5Q_3^2 - 16PQ_1)} \tag{15}$$

We then find that shock-wave solutions exist under the condition $Q_2 + Q_3 = 0$ only in the modulational stability region $PQ_1 < 0$. Using (15), one can express the shock-wave velocity in terms of the asymptotic continuous wave amplitude ρ as follows:

Fig. 9. Wave evolution in modulational instability region for equation parameters $P = 1$, $Q_1 = 1.9716 \times 10^{-3}$, $Q_2 = 0.85439$, and $Q_3 = -0.3079$. Plots of rows (*a*) and (*b*) show the wave evolutions at given times along the *x*-direction and at given point along the *t*-direction, respectively.

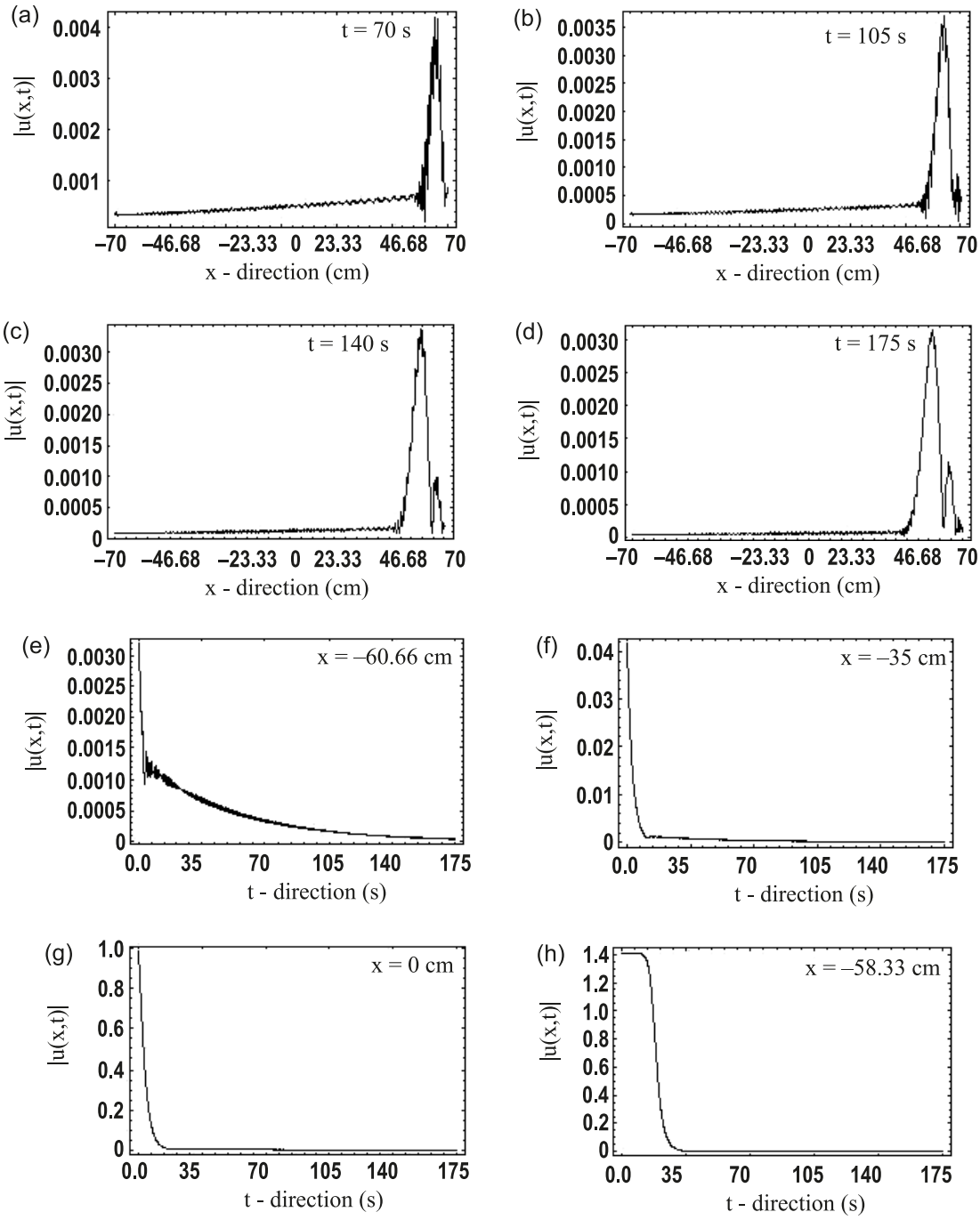

$$V = V(\rho) = -\frac{13(PQ_3 + Q_3 - 4P)\rho^2}{2(3 + 3P + 5Q_3\rho^2)} \tag{16}$$

2. Case $4PQ_1 + Q_2^2 = Q_3 = 0$

In the present case one obtains

$$V = -\frac{P+1}{2} \tag{17}$$

and solution (15) is governed by the two free parameters m and ρ. For the shock-wave velocity to be positive, we must have $P + 1 < 0$. The resulting two-parameter shock-wave solution holds only in the stability ($PQ_1 < 0$) domains. It should be noted that in the present case, the shock-wave velocity does not depend on the asymptotic continuous-wave amplitude ρ; moreover, it is free from Q_1, Q_2, and Q_3..

3. Case $(|4PQ_1 + Q_2^2| + |Q_3|)(Q_2 + Q_3) > 0$

In this case, we have $(Q_2 + Q_3)(4PQ_1 + 4Q_2Q_3 + Q_2^2 + 3Q_3^2) \neq 0$ and

$$m^2 = \frac{b}{2}\rho^2$$
$$\rho^2 = -\frac{6(Q_2+Q_3)V + 3(P+1)(Q_2+3Q_3)}{8(4PQ_1 + 4Q_2Q_3 + Q_2^2 + 3Q_3^2)} \quad (18)$$

where

$$b = [(P+2V+1)Q_2 + (3P+2V+3)Q_3](4P^2)^{-1}$$

and V is any positive solution of the quadratic equation

$$-12(Q_2+Q_3)^2V^2 + 4[(P+1)(32PQ_1 + 20Q_2Q_3 + 5Q_2^2 + 5Q_3^2) + 12P(Q_2+Q_3)]V + 3(P+1)(Q_2+3Q_3)[8P - (P+1)(Q_2+3Q_3)] = 0 \quad (19)$$

To obtain the conditions of validity of solution (13), one may first find the positive solution of (19), secondly insert the expression for V in b and into (18), and lastly, one may impose the condition of positivity of b and ρ^2.

It should be noted that it is also possible to express the shock-wave velocity V in terms of the asymptotic continuous wave amplitude ρ

$$V = V(\rho) = -\frac{4(4PQ_1 + 4Q_2Q_3 + Q_2^2 + 3Q_3^2)}{3(Q_2+Q_3)}\rho^2 - \frac{(P+1)(Q_2+3Q_3)}{2(Q_2+Q_3)} \quad (20)$$

2.3 Some characteristics of the established DSW

The most essential characteristics of the established DSW is the dependence of its velocity V on the parameter ρ and derivative nonlinearities. As mentioned above, the velocity V is independent of ρ and of the derivative nonlinearities in the case $4PQ_1 + Q_2^2 = Q_3 = 0$.

In the case of solution (15) with parameters (13), results demonstrating the (*i*) $V(Q_3)$ and (*ii*) $\rho(Q_3)$ dependence are displayed in Fig. 2*a* for the the parameter values $P = 1$ and $Q_1 = -0.5$. Figure 2*b*, obtained from Fig. 2*a*, shows the dependence of $V(\rho)$ for the above values of the equation parameters. An obvious inference suggested by Fig. 2 is that the dependence $V(\rho)$ or $V(Q_3)$ is neither linear nor monotone. This implies that the derivative nonlinear terms in (1) cannot be neglected. Another conclusion from Fig. 2 is that, depending on the parameter values in the equations, the derivative nonlinearity terms in (1) may either increase or decrease the speed of the shock wave. For the chosen parameter values $P = 1$ and $Q_1 = -0.5$, the asymptotic continuous-wave amplitude increases with the derivative nonlinearity Q_3 and its maximal and minimal values are obtained for $V = 0$, corresponding to two critical values of $Q_3 = 0.42265$ and $Q_3 = 1.5774$, respectively.

Plots of Fig. 3 correspond to the shock-wave solution (15) with parameters (18) and (19). Curves (1) and (2) of Fig. 3*a* show the dependence of V and ρ on Q_3, respectively, while Fig. 3*b* shows the evolution of V versus ρ. The two plots are obtained with the equation parameters $P = 1$ and $Q_1 = -0.5$ when the derivative nonlinearities satisfy the relationship $Q_2 + 3Q_3 = 0$. As in the above case, Fig. 3*b* is obtained from Fig. 3*a*. Neither the shock velocity V nor the asymptotic continuous-wave amplitude ρ is monotone as a function of Q_3 for $-10 \le Q_3 \le 0$, so that for a specific choice of equation parameters, the derivative terms in (1) can either increase or decrease the propagating speed of the shock. The two plots correspond to a shock wave moving in the modulational stability domain ($PQ_1 = -0.5 < 0$).

3. Numerical simulations of the dispersive shock wave

Numerical simulations are carried out on the above exact shock-wave solutions within the framework of the Q-DNLS equation (1). Many sets of the equation parameters are chosen in our simulations. There exist a number of algorithms suitable for the numerical solution of this type of problem but some methods must be used with caution if convergence is to be assured. For now, it should be noted that one of the best-known methods to solve the Q-DNLS equation numerically is the Crank–Nicolson method, as it is stable and accurate to second order in space and time [38]. Hence, the numerical simulations of (1) are performed using this method. The accuracy of our numerical computations is checked by testing different time and space steps. The variables t and x are measured in units of time (second (s)) and space (centimetre (cm)), respectively.

Using the Q-DNLS equation (1) as a model equation of wave propagation in a semi-infinite network it is easy to observe the major features of dispersive shock-wave propagation. Progressive transformation of the initial dispersive shock-wave signal into various type of waves is show in Figs. 4–9. In all these figures, plots in row (*a*) show the wave propagation along the x-direction for different times t, while plots in row (*b*) give the wave propagation along the t-direction for different x.

Plots of Fig. 4 show the wave evolution in the modulational instability region with the input shock signal taken from the first class of shock-wave solutions (4). The equation parameters used are $P = 0.4$, $Q_1 = 0.2$, $Q_2 = 1.3$, and $Q_3 = -1$. Plots of row (*a*) show that the waves propagate from the left to the right, while plots of row (*b*) show that the amplitude of the wave decreases as x increases.

In Fig. 5, we showed the wave evolution in the modulational stability zone with the input shock signal taken from the class of shock-wave solutions (4). Equation parameters $P = 0.4$, $Q_1 = -0.2$, $Q_2 = 1.3$, and $Q_3 = -1$ are used. The plots of this Fig. 5 show that the wave amplitude decreases as x increases.

To show that the wave amplitude decreases as time increases, we plot, in Figs. 6 and 7, the wave profile in the modulational stability and modulational instability regions, respectively. For these plots, we used the exact dispersive shock-wave solution (4) for the input signal. Plots of Fig. 6 are obtained with the same equation parameters as in Fig. 5, but with derivative coefficient $Q_3 = -3$. This same value of Q_3 has been used for Fig. 7 where the other equation parameters are the same as in Fig. 4. These two figures, Figs. 6 and 7, show that the amplitude of the wave decreases as a function of time t when it propagates either in the modulational stability region or in the modulational instability region. Figures 6 and 7 also show how much the derivative

parameter Q_3, and consequently the derivative coefficients $Q_2 + 2Q_3$ and Q_3 of (1) affect the wave amplitude: Comparing the plots of Figs. 4 and 5 with those of Figs. 7 and 6, respectively, it is seen that the wave amplitude increases as the derivative coefficient Q_3 decreases (for Figs. 4 and 5, we took $Q_3 = -1$ while $Q_3 = -3$ was used for Figs. 6 and 7). It is also seen from the plots of Figs. 4–7 that the wave amplitude slowly decreases as function of space variable x when Q_3 decreases (compare the plots of rows (*b*) of Figs. 4 and 5 with those of Figs. 7 and 6, respectively). Finally, a simple comparison of Figs. 4 and 5 with Figs. 7 and 6, respectively, shows that the DSW oscillates more as Q_3 decreases.

In Figs. 8 and 9 we present the numerical solutions of (1) obtained with the use of solution (13) for the input signal, but with different equation parameters. For Fig. 8, we used $P = 2$, $Q_1 = -27$, $Q_2 = -2$, and $Q_3 = 2$, while for Fig. 9 we used $P = 1$, $Q_1 = 1.9716 \times 10^{-3}$, $Q_2 = 0.85439$, and $Q_3 = -0.3079$. These two sets of equations parameters satisfy condition (14) and (15) and condition (18) and (19), respectively. Therefore Figs. 8 and 9 show the wave propagation in modulational stability region and in modulational instability region, respectively. These two figures show that the wave amplitude decreases as function of time t (see plots of column (*a*)) and increases as function of x (see plots of column (*b*)) when the input signal is taken from the second class of dispersive shock-wave solution (13).

The combined action of dispersion and derivative nonlinearity in (1) leads to the generation of an expanding nonlinear oscillatory structure. This fact is confirmed by numerical plots in Figs. 6–9, which present oscillatory structure of stable dispersive shock wave propagating in either the modulational stability region or modulational instability zone. From these figures, it is seen that dispersive shock waves of (1) are generated which manifest themselves as undular structures [39].

4. Conclusion

In this work we have studied dispersive shock waves in a derivative cubic-quintic nonlinear Schrödinger equation without dissipative term, which is derived in the small-amplitude and long-wavelength limit using the standard reductive perturbation technique and complex expansion, and can describe wave propagation in nonlinear electrical transmission lines. Seeking for dispersive shock-wave solutions of the equation, we found that the derivative nonlinearity terms in the equation is responsible for dispersive shock-wave propagation in the network. Using the exact dispersive shock-wave solutions as input signal, wave propagation in semi-infinite network has been numerically investigated. The numerical study shows that dispersive shock waves manifest themselves as undular structures.

References

1. R. Hirota and K. Suzuki. J. Phys. Soc. Jpn. **28**, 1366 (1970). doi:10.1143/JPSJ.28.1366.; Proc. IEEE, **61**, 1483 (1973). doi:10.1109/PROC.1973.9297.
2. M. Remoissenet. Waves called solitons. 3rd ed. Springer-Verlag, Berlin. 1999.
3. A.C. Scott. Active and nonlinear wave propagation in electronics. Wiley-Interscience, New York. 1970.
4. J. Sakai and T. Kawata. J. Phys. Soc. Jpn. **41**, 1819 (1976). doi:10.1143/JPSJ.41.1819.
5. T. Yagi and A. Noguchi. Electron. Commun. Jpn. **59A**, 1 (1976).
6. E. Kengne, V. Bozic, M. Viana, and R. Vaillancourt. Phys. Rev. E: Stat. Nonlin. Soft Matter Phys. **78**, 026603 (2008). PMID:18850958.
7. P. Marquié, J.M. Bilbault, and M. Remoissenet. Phys. Rev. E: Stat. Phys. Plasmas Fluids Relat. Interdiscip. Topics, **49**, 828 (1994). PMID:9961275.
8. E. Seve, P. Tchofo Dinda, G. Millot, M. Remoissenet, J.M. Bilbault, M. Haelterman, and M. Haelterman. Phys. Rev. A, **54**, 3519 (1996). doi:10.1103/PhysRevA.54.3519. PMID: 9913880.
9. T. Taniuti and H. Washimi. Phys. Rev. Lett. **21**, 209 (1968). doi:10.1103/PhysRevLett.21.209.
10. T.B. Benjamin and J.E. Feir. J. Fluid Mech. **27**, 417 (1967). doi:10.1017/S002211206700045X.
11. K.E. Lonngren. Solitons in action. *Edited by* K.E. Lonngren and A.C. Scott. Academic, New York. 1978.
12. A. Hasegawa. Phys. Rev. Lett. **24**, 1165 (1970). doi:10.1103/PhysRevLett.24.1165.; Phys. Fluids, **15**, 870 (1972). doi:10.1063/1.1693996.
13. P. Marquié, J.M. Bilbault, and M. Remoissenet. Phys. Rev. E: Stat. Phys. Plasmas Fluids Relat. Interdiscip. Topics, **51**, 6127 (1995). PMID:9963352.
14. E. Kengne and R. Vaillancourt. Commun. Nonlinear Sci. Numer. Simul. **14**, 3804 (2009). doi:10.1016/j.cnsns.2008.08.016.
15. E. Kengne and R. Vaillancourt. J. Infrared Millimeter Waves, **30**, 679 (2009). doi:10.1007/s10762-009-9485-7.
16. E. Kengne, R. Vaillancour, and B.A. Malomed. Int. J. Mod. Phys. B, **23**, 133 (2009). doi:10.1142/S0217979209049887.
17. D. Yemélé, P. Marquié, and J.M. Bilbault. Phys. Rev. E: Stat. Nonlin. Soft Matter Phys. **68**, 016605 (2003). PMID: 12935268.
18. E. Kengne. J. Phys. Math. Gen. **37**, 6053 (2004). doi:10.1088/0305-4470/37/23/007.
19. E. Kengne, S.T. Chui, W.M. Liu, and W.M. Liu. Phys. Rev. E: Stat. Nonlin. Soft Matter Phys. **74**, 036614 (2006). PMID: 17025771.
20. E. Kengne and W.M. Liu. Phys. Rev. E: Stat. Nonlin. Soft Matter Phys. **73**, 026603 (2006). PMID:16605467.
21. T. Taniuti and N. Yajima. J. Math. Phys. **10**, 1369 (1969). doi:10.1063/1.1664975.
22. R.J. Deissler and H.R. Brand. Phys. Lett. **146A**, 252 (1990).
23. M. Marklund and P.K. Shukla. Phys. Rev. E: Stat. Nonlin. Soft Matter Phys. **73**, 057601 (2006). PMID:16803083.
24. M. Hoefer and M. Ablowitz. Dispersive shock waves, http://www.scholarpedia.org/article/Dispersive_shock_waves.
25. G.A. El, R.H.J. Grimshaw, and N.F. Smyth. Phys. Fluids, **18**, 027104 (2006). doi:10.1063/1.2175152.
26. G.B. Whitham. Linear and nonlinear waves. Wiley-Interscience, New York. 1974.
27. R.Z. Sagdeev. Collective processes and shock waves in rarified plasma. *In* Problems of plasma theory. Vol. 5. *Edited by* M.A. Leontovich. Atomizdat, Moscow. 1964.
28. D. Krökel, N.J. Halas, G. Giuliani, and D. Grischkowsky. Phys. Rev. Lett. **60**, 29 (1988). doi:10.1103/PhysRevLett.60.29. PMID:10037859.
29. B.L. Holian and G.K. Straub. Phys. Rev. B, **18**, 1593 (1978). doi:10.1103/PhysRevB.18.1593.; B.L. Holian, H. Flaschka, and D.W. McLaughlin. Phys. Rev. A, **24**, 2595 (1981). doi:10.1103/PhysRevA.24.2595.; D.J. Kaup. Physica D, **25**,

361 (1987). doi:10.1016/0167-2789(87)90109-6.; S. Kamvissis. Physica D, **65**, 242 (1993). doi:10.1016/0167-2789(93)90161-S.
30. M.A. Hoefer, M.J. Ablowitz, I. Coddington, E.A. Cornell, P. Engels, and V. Schweikhard. Phys. Rev. A, **74**, 023623 (2006). doi:10.1103/PhysRevA.74.023623.
31. J.J. Chang, P. Engels, and M.A. Hoefer. Phys. Lett. Rev. **101**, 170404 (2008). doi:10.1103/PhysRevLett.101.170404.
32. A.M. Kamchatnov. Nonlinear periodic waves and their modulations — An introductory course. World Scientific, Singapore. 2000.
33. M.A. Hoefer and M.J. Ablowitz. Physica D, **236**, 44 (2007); G.A. El and R.H.J. Grimshaw. Chaos, **12**, 1015 (2002). doi:10.1063/1.1507381. PMID:12779625.
34. K. Nozaki and N. Bekki. Phys. Rev. Lett. **51**, 2171 (1983). doi:10.1103/PhysRevLett.51.2171.
35. D. Kong. Phys. Lett. **196A**, 301 (1995).
36. B. Dey, A. Khare, and C.N. Kumar. Phys. Lett., **223A**, 449 (1996). doi:10.1016/S0375-9601(96)00772-4.
37. S.N. Behera and A. Khare. Pramana – J. Phys. **15**, 245 (1980). doi:10.1007/BF02847222.
38. W.H. Press, B.P. Flannery, S.A. Teukolsky, and W.T. Vallerling. Numerical recipes in Fortran. Cambridge University Press, Cambridge. 1992.
39. A.J. Colosi, C.R. Beardsley, F.J. Lynch, G. Gawarkiewicz, C.-S. Chiu, and A. Scotti. J. Geophys. Res. **106**, C5, 9587 (2001). doi:10.1029/2000JC900124.